Finite Control Set Model Predictive Control Combined with Online Junction Temperature Estimation for Reliability Enhancement of Voltage Source Inverters

Qiang Mu, Jiale Zhou, Zaheen Mustakin, Lucas Pereira, Babak Parkhideh, Tiefu Zhao
Dept. of Electrical and Computer Engineering
Energy Production and Infrastructure Center (EPIC)
University of North Carolina at Charlotte
Charlotte, NC, USA
qmu1@charlotte.edu; jzhou20@charlotte.edu;
zmustaki@charlotte.edu; lpereira@charlotte.edu;
bparkhideh@charlotte.edu; tzhao5@charlotte.edu

***Abstract*—As the efficiency of the power converter has significantly improved, its long-term reliable operation has become a critical factor in most power electronics applications. Among these factors, monitoring real-time temperature variations in the power converter during operation is a key priority for assessing reliability and predicting its lifetime. However, limited research has been conducted on the online monitoring of junction temperatures in power semiconductors using on-resistance measurements. Online temperature monitoring can help prevent individual device failure caused by transient thermal overstress, which could otherwise undermine the reliability of the entire converter. The power semiconductor junction temperature prediction method discussed in this paper still relies on the less commonly used direct measurement of on-resistance. Building on this approach, a combined method is proposed that integrates finite control set model predictive control (FCS-MPC) to minimize power loss and thermal stress in power semiconductors, thereby improving the overall reliability of the converter. Above all, acknowledging the variations in parameter distribution among identical power semiconductor devices, this method aims to estimate the online junction temperatures of all SiC power MOSFETs in a three-phase, two-level voltage source inverter. The simulation results demonstrate that the proposed method enables online estimation of the junction temperature of all SiC power MOSFETs in a three-phase inverter, and even allows closed-loop regulation of the junction temperature of the SiC power MOSFETs. Simultaneously, the reliability of the power MOSFET is notably enhanced due to the considerable reduction in junction temperature achieved by the proposed method. In addition, the single-vector MPC under finite set model predictive control, along with the double-vector and triple-vector approaches under continuous set model predictive control, are used for comparative analysis with the proposed method. After comparison, the excellence of the proposed method was finally verified through simulation.**

Keywords—junction temperature, on-resistance, voltage source inverter, model predictive control (MPC), single-vector, double-vector, triple-vector, reliability assessment.

I. Introduction

The voltage source inverter is widely used in renewable energy generation, energy storage, uninterruptible power supply and electric vehicle drive systems, mainly due to its simple design [1-2]. With significant improvements in the efficiency of the voltage source inverter, its long-term reliable operation has become a crucial factor in most power electronics applications. Power semiconductors are recognized as one of the most vulnerable components in power converters, with their failure rate closely correlated to the junction temperature during operation. Thus, it is essential to keep these temperatures within safe limits. Despite considerable efforts by the scientific community and power module manufacturers, accurately measuring the junction temperature of power semiconductor devices continues to be a challenge. Effective thermal management of SiC devices is especially challenging due to their low thermal inertia and high power density. One way to prevent temperature-related failures is by estimating junction temperatures, which allows for precise thermal management and improves converter reliability. Over time, several methods have been developed to measure or estimate the junction temperature of power semiconductors. As noted in [3], current methods for estimating the temperature of power semiconductor devices can be broadly classified into optical, physical contact, and electrical methods, each offering distinct advantages and disadvantages. Optical methods involve detecting the temperature-dependent optical properties of semiconductors, such as through thermal imaging of the semiconductor die with infrared cameras [4-8]. These methods offer high accuracy and produce detailed thermal images of the semiconductor die, allowing for easy identification of the maximum temperature point and the temperature gradient across the die. However, these methods require visual access to the chip, removal of the dielectric gel, and additional computational resources to analyze the thermal images. Physical contact methods involve making direct contact between the die and a heat-sensitive material. This approach necessitates mechanical contact with the die inside the module and typically provides limited accuracy and dynamic response.

979-8-3315-1611-6/25/$31.00 ©2025 IEEE

Electrical methods, especially those utilizing thermosensitive electrical parameters (TSEPs), have emerged as the most promising approach for estimating junction temperature in power semiconductors. These methods use the power semiconductor device itself as a temperature sensor, converting its junction temperature into electrical variables. TSEPs in SiC MOSFETs can be categorized into transient and steady-state groups. Transient TSEPs include parameters such as turn-on saturation current [9], turn-on or turn-off delay [10-11], internal gate resistance [12], and gate threshold voltage (V_{th}) [13-15]. Steady-state TSEPs mainly refer to parameters like on-state voltage (V_{on}) [16-17] and on-resistance (R_{dson}) [18-20]. Additionally, some transient TSEPs have been proposed, including turn-on drain-source current overshoot [21], turn-off drain-source voltage undershoot [22], and gate current [23]. Notably, V_{dson} and the on-state voltage drop of the body diode (V_{bdon}) are often combined as indicators of junction temperature (T_j) [24]. Among the various TSEPs, the relationship between on-resistance (R_{dson}) and junction temperature in MOSFETs is especially reliable and practical. This correlation enables direct estimation of T_j, facilitating real-time temperature monitoring to prevent individual device failures caused by transient thermal overstress, thus improving the reliability of the entire converter. Therefore, this paper uses on-state resistance (R_{dson}) as an indicator for the online junction temperature of power semiconductor devices.

At the same time, based on the successful online monitoring of junction temperature, it is still necessary to combine some advanced control methods to improve the reliability of the converter. Thermal stress has been identified as one of the main causes of failure in power modules. The thermal stress caused by power loss can accelerate the degradation of semiconductor devices and reduce system reliability. Adjusting the switching frequency is the most straightforward method for achieving thermal control, as it directly affects power switching losses. MPC, a nonlinear control technology, has received more attention due to its advantages of flexible control and simple implementation [25-26]. A converter topology with a specific level has a limited number of switching states; therefore, MPC heuristically selects the best switching state from the possibilities by minimizing an objective function. At present, few scholars have studied the method of using MPC to improve reliability [27]. Although FCS-MPC was used in combination with on-site junction temperature to improve reliability in [28], it did not take into account the parameter differences of semiconductor devices that lead to junction temperature differences**.** Therefore, acknowledging the variations in parameter distribution among identical power semiconductor devices, this study aims to estimate the online junction temperatures of all SiC power MOSFETs in a three-phase, two-level voltage source inverter. Additionally, while monitoring the online junction temperature of power semiconductor devices, the finite control set model predictive control method can be applied further by incorporating power loss as a secondary objective within the control function. This approach helps reduce power loss in semiconductor devices, thereby minimizing their thermal stress.

This paper presents an FCS-MPC method integrated with online junction temperature prediction to limit the rise in

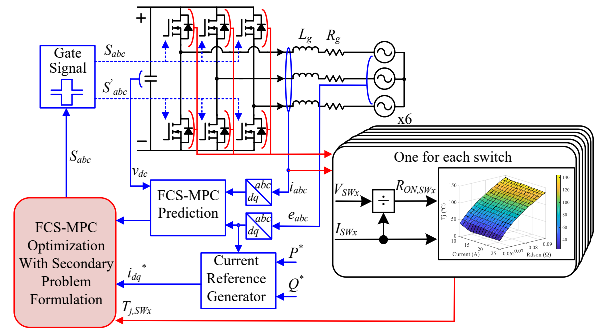

Fig. 1. Finite control set model predictive control diagram with online junction temperature estimation.

junction temperature of power devices, thereby improving the reliability of the entire converter. The proposed method enables online estimation of the junction temperatures for all silicon carbide (SiC) power MOSFETs in a three-phase inverter and even allows closed-loop regulation of the junction temperature of the SiC power MOSFETs.

II. The Proposed Finite Control Predictive Control Method With Online Junction Temperature Estimation

Fig. 1 illustrates finite control set model predictive control diagram combined with online junction temperature estimation. It mainly includes two parts: FCS-MPC and online junction temperature estimation. In the FCS-MPC framework, the primary objective is to implement power flow control, while the secondary objective focuses on minimizing power loss, which is determined using the power loss model of semiconductor devices. The secondary problem formulation, which employs a similar l_2 norm-2 least squares objective function for power loss, is presented as follows [29]:

$$J_s = \sum_{j=1}^{H} ||0\text{-}E_{abc}[k+j]||_2^2 \tag{1}$$

Here, 0 represents the reference power loss, E_{abc} represents the power loss calculated using the loss model, and J_s corresponds to the secondary objective. Thus, the combined objective function, which integrates power flow control and power loss reduction, is expressed as follows:

$$\min_{S_{abc}} \lambda_p \cdot J_p + \lambda_s \cdot J_s \tag{2}$$

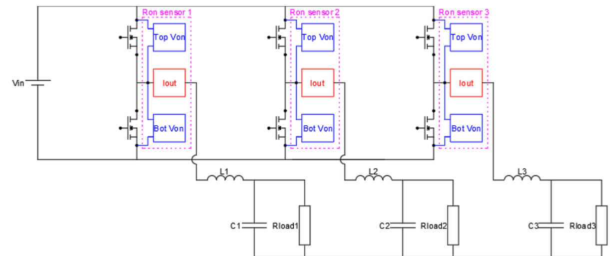

Fig. 2. Three-phase voltage source inverters architecture with proposed $R_{ds\text{-}on}$ estimation architecture and package.

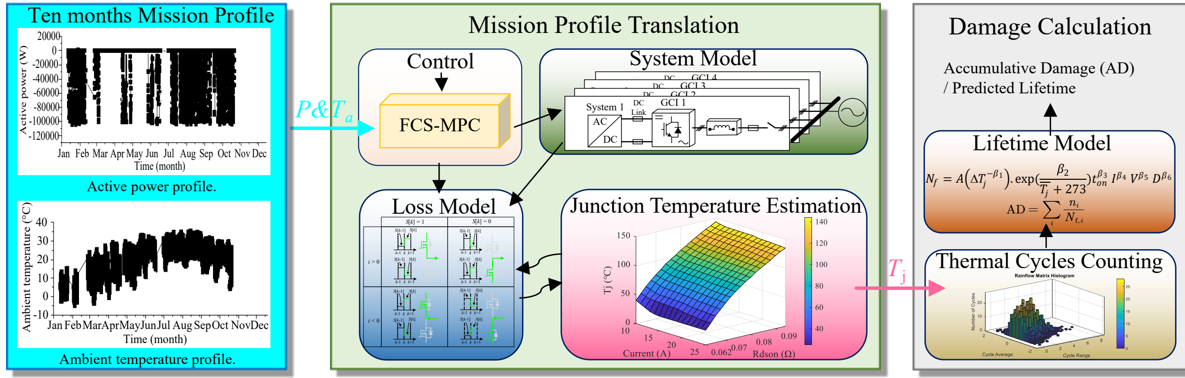

Fig. 3. Reliability assessment framework of semiconductor for voltage source inverter inverters using the proposed method [30].

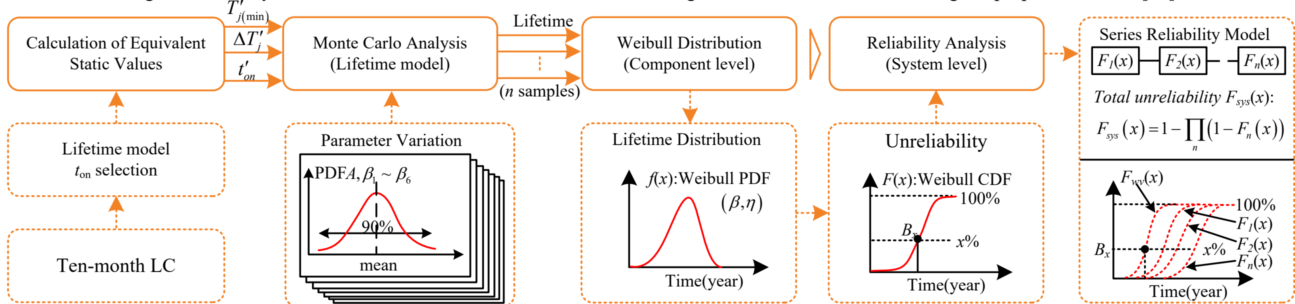

Fig. 4. Flow diagram of the reliability assessment of SiC inverters with the Monte Carlo analysis and reliability block diagram. LC: lifetime consumption, t_{on}: heating time, T_j(min): equivalent minimum junction temperature, $\Delta T'_j$: equivalent cycle amplitude, t'on: equivalent heating time, $f(x)$: Weibull Probability density function (PDF), β: sharp parameter, η: scale parameter, $F(x)$: cumulative density function (CDF), $F_i(x)$: unreliability function of the ith device in the system, $F_{sys}(x)$: total unreliability of the system, and B_x : operation time when x% of the populations fail [31].

Here, S_{abc} represents the switching state of the power semiconductor devices, J_p denotes the primary objective value for power flow control, and λ_p and λ_s are the weighting factors for the primary and secondary objective functions, respectively. λ_p is set to 1 by default here. The value of λ_s will be selected based on the requirements of the specific application.

For the online junction temperature estimation part, to measure the junction temperature online, ultrafast sensors are used to monitor the on-state current and voltage of all power devices. In [32], the traditional method of measuring $R_{ds\text{-}on}$ requires each phase bridge arm's upper and lower power devices to have their own voltage sensors, while the current of the power device is determined using the output current sensor. However, this approach lacks better sensor integration and involves more complex isolation of power supplies. Figure 2 illustrates the design of three-phase voltage source inverters architecture with proposed $R_{ds\text{-}on}$ estimation architecture and package. The proposed $R_{ds\text{-}on}$ estimation architecture forms a standalone package by positioning the current sensor between the voltage sensors of the upper and lower power devices, effectively addressing the integration and isolation power supply challenges associated with the traditional method. These measurements are then fed into a lookup table, created from double pulse tests in [28], which defines on-resistance as a function of junction temperature and conduction current. If all semiconductor devices were to be tested, the workload required in practice would be too large. This paper aims to verify the proposed control method; therefore, only a single power semiconductor is tested, and the corresponding mapping is obtained. The remaining mappings are derived from the obtained data by making minor adjustments to generate all the mappings. The junction temperature is subsequently determined online during operation by referencing this lookup table, based on the real-time sampled conduction current and voltage of the device. Finally, the junction temperature of all SiC power MOSFETs, derived from the lookup table, is integrated into the previously analyzed secondary objective function of the FCS-MPC, enabling the closed-loop regulation of their junction temperatures.

III. Reliability Assessment Based on The Proposed Method

The reliability assessment framework is illustrated in Fig. 3, is based on the real-world mission profiles of the PV system in North Carolina. The field data has been processed to create the mission profile, which serves as the input for the reliability assessment framework. To translate the mission profile between the input and output of the framework, control methods, system models, loss models, and junction temperature estimation are required. The framework outputs the accumulative damage or predicted lifetime of the semiconductors. The quantified

Table I - Equivalent Static Values Of The Stress Parameters

Mean junction temperature T'_{jm}	21.8°C
Cycle amplitude $\Delta T'_j$	0.1741°C
Cycle period t'_{on}	0.01s
Number of cycles per ten-month n'_i	(10×30×24×60×60)×50

TABLE II - SIMULATION PARAMETERS

Symbol	Parameters	Values
P	Rated power	20 kW
V_{dc}	DC-link voltage	1200 V
e_{abc}	Grid voltage	277/480 V
f	Grid frequency	60 Hz
i_{abc}	Grid current	24 A
L_g	Line inductance	20 mH
R_g	Line resistance	10 mΩ
MOSFET	Semiconductor device	C2M0080120D
T_a	Air temperature	25 ℃
$R_{\theta AH}$	Thermal resistance from air to heatsink	0.5 ℃/W
$R_{\theta HC}$	Thermal resistance from heatsink to case	0.5 ℃/W

accumulative damage is closely associated with the semiconductor specifications, PV inverter topology, and control methods. The results are representative and will be further refined upon receiving the detailed design and specifications from the inverter vendor. The framework serves as a universal tool for quantitatively comparing the reliability of PV inverters from different vendors employing various control methods. Based on the ten-month lifetime of the power device calculated above, it can be concluded that the lifetime of the corresponding power device is a fixed value. This often deviates from reality because variations in device parameters and thermal stresses are not accounted for [33]. In practice, these uncertainties can cause the lifetime of power devices to vary within a specific range [34]. Therefore, lifetime predictions are typically expressed as statistical values rather than fixed values. Building on the analysis above, a statistical approach utilizing Monte Carlo analysis is applied, as illustrated in Fig. 4. Table I summarizes the equivalent static values derived from the mission profile.

IV. SIMULATION RESULTS

To validate the effectiveness of the proposed finite predictive control method with online junction temperature estimation, simulations are performed comparing the proposed method with single-vector MPC under finite set model predictive control, the double-vector and triple-vector approaches under continuous set model predictive control, using the MATLAB and PLECS environments. The three traditional modulated MPC strategies mentioned above are not the focus of this paper; further details on these methods can be found in [35]. The primary simulation parameters are listed in Table II. Furthermore, to minimize the data volume in the mission profile, the ambient temperature profile is kept constant, the ambient temperature profile is kept constant, while the active power profile is scaled down to a maximum limit of 20 kW. Simultaneously, it is assumed that the mission profile repeats annually. The simulation parameters of the lifetime model are selected from Table III.

TABLE III - SIMULATION PARAMETERS OF THE LIFETIME MODEL

V	1200	Blocking voltage
A	$9.34*10^{14}$	Technology factor
I	300	Current per wire bond
D	$150*10^{-5}$	Diameter of bonding wire
β_1	-4.416	Contribution of Coffin-Manson law
β_2	1285	Contribution of Arrhenius law
β_3	-0.463	Influence of transient thermal response on the chip
β_4	-0.716	Contribution of accelerated wire bonds failure close to end of life
β_5	-0.761	Accounted correlation between blocking voltage and chip thickness
β_6	-0.19	Considered impact of wire diameter on bond interface and thermal expansion

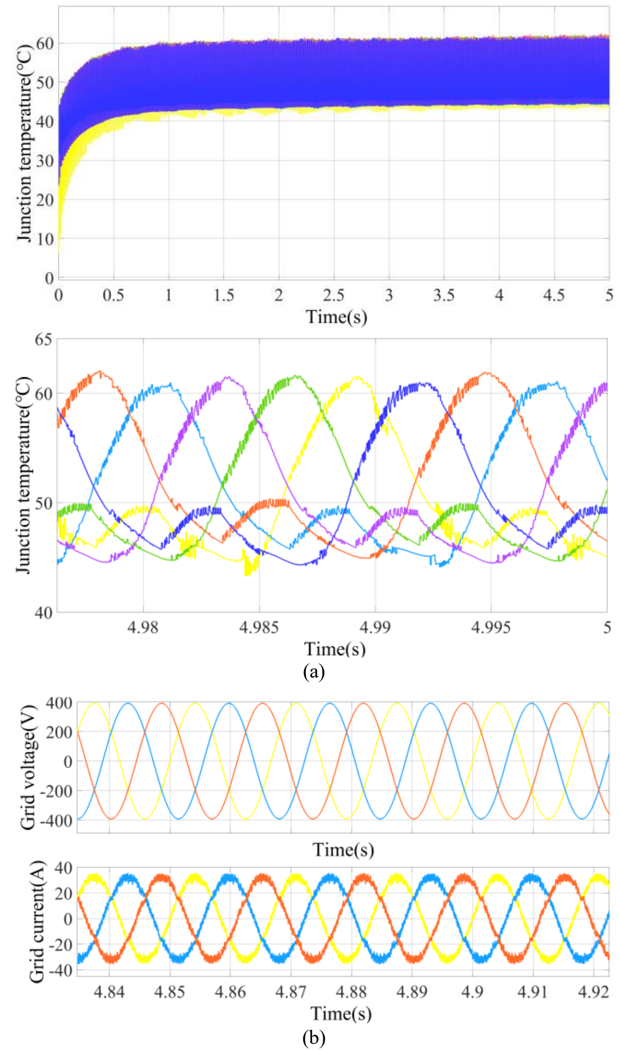

Fig. 5. (a) The junction temperature of all MOSFETs and corresponding zoom-in details (b) Grid voltage and current (Sampling period T_s=33μs, weighting factor $\lambda_s = 250*10^4$).

As illustrated in Figure 5, when the grid voltage and current operate under normal conditions, the six power MOSFETs with varying on-resistances exhibit nearly identical junction temperatures, with a maximum value of approximately 60°C. A closer examination of their junction temperature details reveals that the maximum temperature difference among them does not exceed 1°C. Therefore, the proposed method enables the online estimation of junction temperatures for all SiC power MOSFETs in a three-phase voltage source inverter and facilitates the closed-loop regulation of their junction temperatures by

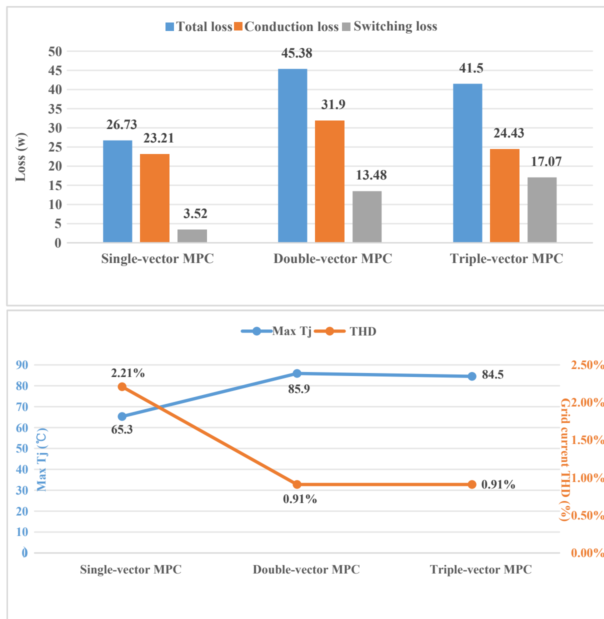

(a)

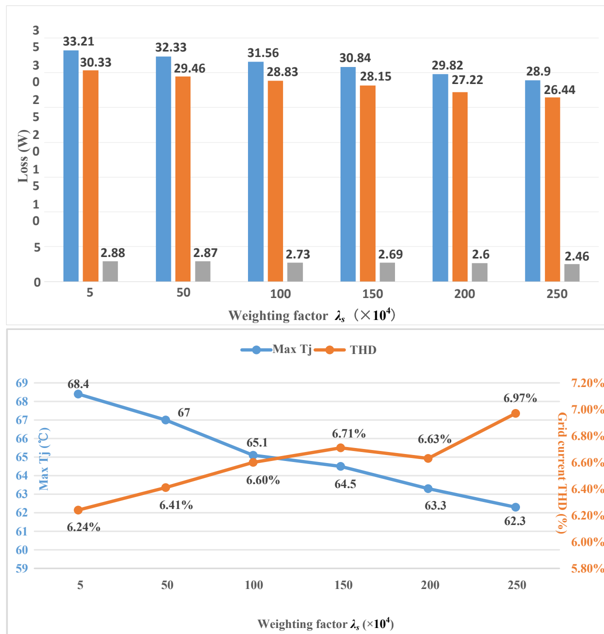

(b)

Fig. 6. Quantitative comparison of different control strategies (a) Other modulated MPC methods (b) Proposed method (T_s=33μs).

incorporating the junction temperature into the previously analyzed secondary objective function of the FCS-MPC. A comparison between the proposed method and conventional modulated MPC methods is shown in Fig. 6. It is evident that, with the proposed method, as the weighting factor increases, the maximum junction temperature of the power semiconductor decreases, achieving lower values compared to other methods. For instance, when the weighting factor λ_s is set to 250, the maximum junction temperature of the power MOSFETs is 3°C lower than that achieved by the traditional single-vector MPC.

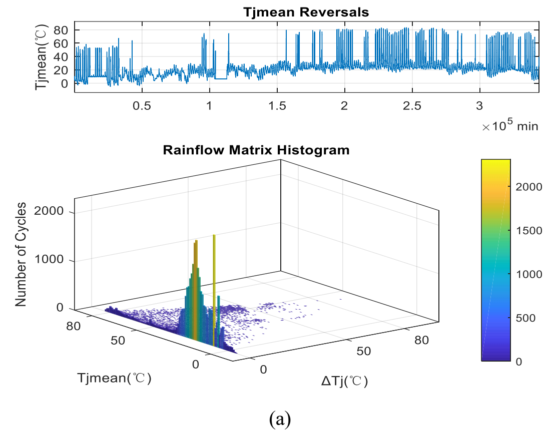

(a)

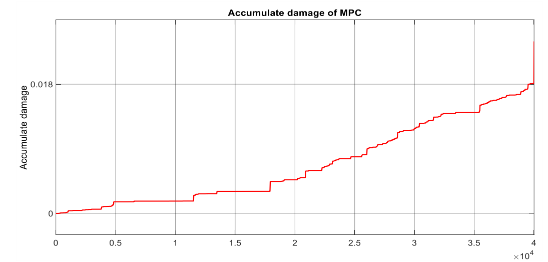

(b)

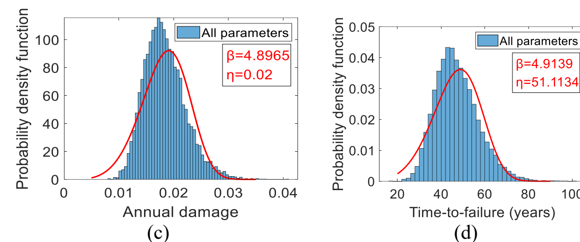

(c) (d)

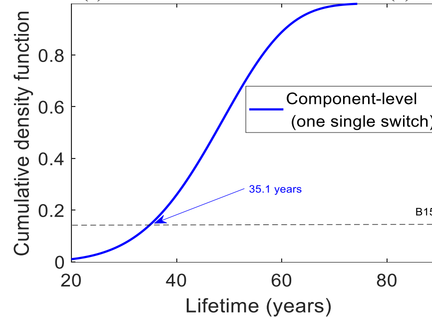

(e)

Fig. 7. Reliability assessment based on the proposed method (a) Rainflow counting results (b) Accumulative damage results (c) Annual damage; (d) Time-to-failure distribution; (e) Cumulative density function along with the lifetime (Ts=25μs, λs = 5*10^4).

Therefore, the reliability of the converter is significantly enhanced. However, the THD of grid current correspondingly increases. Nevertheless, if reliability improvement is prioritized, the proposed method demonstrates superior performance. Simultaneously, it is observed that although the double-vector and triple-vector MPC methods are compared at the same fixed switching frequency, theoretical analysis indicates that the triple-vector MPC incurs higher switching losses due to its use

of additional vectors. However, its conduction loss is lower than that of the corresponding double -vector MPC. Additionally, while the theoretical THD value for the triple-vector method is expected to be higher than that of the double-vector method, at higher switching frequencies, the change in THD becomes negligible or remains unchanged.

Based on the previous reliability analysis, the component-level unreliability functions of the converters are presented in Fig. 7, along with their corresponding component-level B_{15} lifetimes. FCS-MPC, as a nonlinear control algorithm, selects the optimal switching state from a finite set of candidates by minimizing the objective function. As a result, the system-level B_{15} lifetime does not reflect uniform unreliability across all power devices. Specifically, the component-level B_{15} lifetime for the MOSFET under the proposed method is 35.1 years.

V. Conclusion

In this article, a finite control set model predictive control (FCS-MPC) scheme combined with online junction temperature estimation is proposed. The simulation results indicate that the proposed method facilitates the online estimation of junction temperatures for all SiC power MOSFETs in a three-phase inverter, enabling the closed-loop regulation of their junction temperatures. Additionally, the method significantly enhances the reliability of power MOSFETs by substantially reducing their junction temperatures, but it sacrifices the corresponding THD of the grid current. Finally, the superiority of the proposed method is verified by comparing it with the single-vector MPC under finite set model predictive control, and the double-vector and triple-vector MPC methods under continuous set model predictive control. This paper lays the foundation for better applying MPC algorithm to reliability improvement projects in the future.

References

[1] J. Teng, X. Sun, M. Zhang, W. Zhao and X. Li, "Low-Capacitance CHB-Based SST Based on Resonant Push–Pull Decoupling Channel," in *IEEE Transactions on Industrial Electronics*, vol. 71, no. 3, pp. 2477-2488, March 2024.

[2] Z. Wang *et al*., "Common-Mode Voltage Suppression Strategy for CHB-Based Motor Drive Based on Topology and Modulation Optimization," in *IEEE Transactions on Power Electronics*, vol. 40, no. 1, pp. 1697-1716, Jan. 2025.

[3] Y. Avenas, L. Dupont and Z. Khatir, "Temperature Measurement of Power Semiconductor Devices by Thermo-Sensitive Electrical Parameters—A Review," in IEEE Transactions on Power Electronics, vol. 27, no. 6, pp. 3081-3092, June 2012.

[4] C. Fang, T. An, F. Qin, X. Bie and J. Zhao, "Study on temperature distribution of IGBT module," 2017 18th International Conference on Electronic Packaging Technology (ICEPT), Harbin, China, 2017.

[5] E. Valor et al., "Comparison of in Situ Land Surface Temperatures Measured with Radiometers and Pyrgeometers: Consequences for Calibration and Validation of Thermal Infrared Sensors," IGARSS 2018 - 2018 IEEE International Geoscience and Remote Sensing Symposium, Valencia, Spain, 2018, pp. 7961-7964.

[6] L. Rossi, G. Breglio, A. Irace and P. Spirito, "Thermal Mapping of Power Devices with a Completely Automated Thermoreflectance Measurement System," 2006 Ph.D. Research in Microelectronics and Electronics, Otranto, Italy, 2006, pp. 41-44.

[7] O.Olanrewaju, Z. Yang, N. Evans, A. Fayyaz, T. Lagier and A. Castellazzi, "Investigation of Temperature Distribution in SIC Power Module Prototype in Transient Conditions," 2019 20th International Symposium on Power Electronics (Ee), Novi Sad, Serbia, 2019, pp. 1-5.

[8] L. Dupont, Y. Avenas and P. -O. Jeannin, "Comparison of Junction Temperature Evaluations in a Power IGBT Module Using an IR Camera and Three Thermosensitive Electrical Parameters," in IEEE Transactions on Industry Applications, vol. 49, no. 4, pp. 1599-1608, July-Aug. 2013.

[9] H. -C. Yang, R. Simanjorang and K. Y. See, "A Method for Junction Temperature Estimation Utilizing Turn-on Saturation Current for SiC MOSFET," 2018 International Power Electronics Conference (IPEC-Niigata 2018 -ECCE Asia), Niigata, Japan, 2018, pp. 2296-2300.

[10] F. Yang, S. Pu, C. Xu, and B. Akin, "Turn-on Delay Based Real-Time Junction Temperature Measurement for SiC MOSFETs With Aging Compensation," in IEEE Transactions on Power Electronics, vol. 36, no. 2, pp. 1280-1294, Feb. 2021.

[11] Z. Zhang et al., "Online Junction Temperature Monitoring Using Intelligent Gate Drive for SiC Power Devices," in IEEE Transactions on Power Electronics, vol. 34, no. 8, pp. 7922-7932, Aug. 2019.

[12] H. Niu and R. D. Lorenz, "Sensing Power MOSFET Junction Temperature Using Gate Drive Turn-On Current Transient Properties," in IEEE Transactions on Industry Applications, vol. 52, no. 2, pp. 1677-1687, March-April 2016.

[13] X. Jiang et al., "Online Junction Temperature Measurement for SiC MOSFET Based on Dynamic Threshold Voltage Extraction," in IEEE Transactions on Power Electronics, vol. 36, no. 4, pp. 3757-3768, April 2021.

[14] B. Strauss and A. Lindemann, "Measuring the junction temperature of an IGBT using its threshold voltage as a temperature sensitive electrical parameter (TSEP)," 2016 13th International Multi-Conference on Systems, Signals & Devices (SSD), Leipzig, Germany, 2016, pp. 459-467.

[15] M. Du, Y. Tang, M. Gao, Z. Ouyang, K. Wei and W. G. Hurley, "Online Estimation of the Junction Temperature Based on the Gate Pre-Threshold Voltage in High-Power IGBT Modules," in IEEE Transactions on Device and Materials Reliability, vol. 19, no. 3, pp. 501-508, Sept. 2019.

[16] M. Guacci, D. Bortis and J. W. Kolar, "On-state voltage measurement of fast switching power semiconductors," in CPSS Transactions on Power Electronics and Applications, vol. 3, no. 2, pp. 163-176, June 2018.

[17] Y. Zhang and Y. C. Liang, "A simple approach on junction temperature estimation for SiC MOSFET dynamic operation within safe operating area," 2015 IEEE Energy Conversion Congress and Exposition (ECCE), Montreal, QC, Canada, 2015, pp. 5704-5707.

[18] Q. Zhang, G. Lu, Y. Yang and P. Zhang, "A High-Frequency Online Junction Temperature Monitoring Method for SiC mosfets Based on on-State Resistance With Aging Compensation," in IEEE Transactions on Industrial Electronics, vol. 70, no. 7, pp. 7393-7405, July 2023.

[19] A. Koenig, T. Plum, P. Fidler and R. W. De Doncker, "On-line Junction Temperature Measurement of CoolMOS Devices," 2007 7th International Conference on Power Electronics and Drive Systems, Bangkok, Thailand, 2007, pp. 90-95.

[20] J. O. Gonzalez, O. Alatise, J. Hu, L. Ran and P. A. Mawby, "An Investigation of Temperature-Sensitive Electrical Parameters for SiC Power MOSFETs," in IEEE Transactions on Power Electronics, vol. 32, no. 10, pp. 7954-7966, Oct. 2017.

[21] Q. Zhang, G. Lu and P. Zhang, "A High-Sensitivity Online Junction Temperature Monitoring Method for SiC mosfets Based on the Turn-on Drain–Source Current Overshoot," in IEEE Transactions on Power Electronics, vol. 37, no. 12, pp. 15505-15516, Dec. 2022.

[22] Y. Yang, Y. Wu, X. Ding and P. Zhang, "Online Junction Temperature Estimation Method for SiC MOSFETs Based on the DC Bus Voltage Undershoot," in IEEE Transactions on Power Electronics, vol. 38, no. 4, pp. 5422-5431, April 2023.

[23] H. Niu and R. D. Lorenz, "Sensing Power MOSFET Junction Temperature Using Gate Drive Turn-On Current Transient Properties," in IEEE Transactions on Industry Applications, vol. 52, no. 2, pp. 1677-1687, March-April 2016.

[24] Q. Zhang, W. Li and P. Zhang, "An Online Junction Temperature Estimating Method for SiC MOSFETs Based on Steady-State Features and GPR," in IEEE Transactions on Industrial Electronics, vol. 71, no. 10, pp. 13299-13309, Jan. 2024.

[25] Y. Zhang *et al*., "A Robust Predictive Current Control of T-Type Three-Level Power Converters Based on Adaptive Linear Neural

Network," *2023 IEEE 2nd International Power Electronics and Application Symposium (PEAS)*, Guangzhou, China, 2023, pp. 1122-1127.

[26] H. Chen, Z. Zhang, Z. Li, P. Zhang and M. Zhang, "Data-Driven Predictive Current Control for Active Front Ends with Neural Networks," *2022 IEEE 17th Conference on Industrial Electronics and Applications (ICIEA)*, Chengdu, China, 2022, pp. 201-206.

[27] M. -H. Nguyen, s. kwak and S. Choi, "Model Predictive Control Algorithm for Prolonging Lifetime of Three-Phase Voltage Source Converters," in IEEE Access, vol. 11, pp. 72781-72802, 2023.

[28] J. Zhou *et al*., "Finite Control Set Model Predictive Control Based on In-Situ Junction Temperature for Reliability Enhancement of Power Converters," *2023 IEEE 10th Workshop on Wide Bandgap Power Devices & Applications (WiPDA)*, Charlotte, NC, USA, 2023, pp. 1-6.

[29] L. Wang, J. He, T. Han, and T. Zhao, "Finite Control Set Model Predictive Control With Secondary Problem Formulation for Power Loss and Thermal Stress Reductions," in *IEEE Transactions on Industry Applications*, vol. 56, no. 4, pp. 4028-4039, July-Aug. 2020.

[30] Q. Mu, J. Zhou, L. Wang, and T. Zhao. “Universal Reliability Assessment of Inverters in Photovoltaic Systems Based on Real-Field Mission Profiles,” 2024 IEEE Energy Conversion Congress and Exposition (ECCE), Phoenix, AZ, USA, 2024, in press.

[31] J. He, A. Sangwongwanich, Y. Yang and F. Iannuzzo, "Lifetime Evaluation of Three-Level Inverters for 1500-V Photovoltaic Systems," in IEEE Journal of Emerging and Selected Topics in Power Electronics, vol. 9, no. 4, pp. 4285-4298, Aug. 2021.

[32] C. Roy, N. Kim, J. Gafford and B. Parkhideh, "On-State Voltage Measurement of High-Side Power Transistors in Three-Phase Four-Leg Inverter for In-Situ Prognostics," *2021 IEEE Energy Conversion Congress and Exposition (ECCE)*, Vancouver, BC, Canada, 2021, pp. 2770-2776.

[33] K. Kuang, X. Guo, C. Li, X. Li, X. Xi and H. Fang, "A Novel Multiscale Perspective Based Hotspot Temperature Assessment Method for Film Capacitor in DC-Link Applications," in *IEEE Transactions on Industry Applications*, vol. 60, no. 6, pp. 9111-9122, Nov.-Dec. 2024.

[34] K. Kuang, X. Guo, C. Li and X. Li, "A Novel Lifetime Estimation Method and Structural Optimization Design for Film Capacitors in EVs Considering Material Aging and Power Losses," in *IEEE Transactions on Device and Materials Reliability*, vol. 24, no. 3, pp. 365-379, Sept. 2024.

[35] L. Guo, M. Chen, Y. Li, P. Wang, N. Jin and J. Wu, "Hybrid Multi-Vector Modulated Model Predictive Control Strategy for Voltage Source Inverters Based on a New Visualization Analysis Method," in *IEEE Transactions on Transportation Electrification*, vol. 9, no. 1, pp. 8-21, March 2023.